




Article

Innovative Hydrodynamic Disintegrator Adjusted to Agricultural Substrates Pre-treatment Aimed at Methane Production Intensification—CFD Modelling and Batch Tests

Monika Zubrowska-Sudol ¹, Aleksandra Dzido ^{2,*} , Agnieszka Garlicka ¹ , Piotr Krawczyk ², Michał Stępień ², Katarzyna Umiejewska ¹, Justyna Walczak ¹, Marcin Wołowicz ²  and Katarzyna Sytek-Szmeichel ¹

¹ Faculty of Building Services, Hydro and Environmental Engineering, Warsaw University of Technology, 00-653 Warsaw, Poland; monika.sudol@pw.edu.pl (M.Z.-S.); agnieszka_garlicka@o2.pl (A.G.); katarzyna.umiejewska@pw.edu.pl (K.U.); justyna.walczak@pw.edu.pl (J.W.); katarzyna.szmeichel@pw.edu.pl (K.S.-S.)

² Faculty of Power and Aeronautical Engineering, Warsaw University of Technology, 00-655 Warsaw, Poland; piotr.krawczyk@pw.edu.pl (P.K.); michal.stepien.dokt@pw.edu.pl (M.S.); marcin.wolowicz@pw.edu.pl (M.W.)

* Correspondence: aleksandra.dzido.dokt@pw.edu.pl

Received: 8 July 2020; Accepted: 14 August 2020; Published: 17 August 2020



Abstract: The study objective was to adjust the hydrodynamic disintegrator dedicated to sewage sludge pre-treatment (HDS) to work with agricultural substrate. This involved the development and implementation of a mathematical model of flow via the device's domain. An innovative disintegrator (HAD—hydrodynamic disintegrator for agriculture) was designed, built, and tested based on the obtained results. The main improvements to the HDS include the implementation of shredding knives in order to overcome clogging by crushed substrate, and the application of ribs in the recirculation zone, contributing to the development of an additional structure damage zone. The challenge of this study was also to determine the operating parameters of the HDA that would provide for an increase in methane production with positive energy balance. The testing procedures, for which maize silage was selected, involved batch disintegration tests and biochemical methane potential tests. No clogging of rotor or spontaneous shutting off of the device, in other words, problems that had occurred in the HDS, were observed. The applied pre-treatment method permitted an increase in the methane potential of maize silage by 34.4%, 27.0%, and 21.6%, respectively for samples disintegrated at energy densities of 10 kJ/L, 20 kJ/L, and 35 kJ/L with net energy profit.

Keywords: agricultural substrates; hydrodynamic disintegration; computational fluid dynamic; mathematical modelling; immersed solid method; cavitation; specific methane production; energy balance

1. Introduction

In December 2018, the Renewable Energy Directive (Directive (EU) 2018/2001) became effective as part of the Clean Energy for All Europeans package. Its purpose is to maintain the EU's position as a global leader in the field of renewable energy sources, and in a broader context to help the European Union meet its emission reduction commitments. The new directive sets a binding target according to which by 2030 at least 32% of the final energy consumption in the European Union should be obtained from renewable sources [1].

Today, the EU aims to have achieved a 20% share of renewable energy in gross final energy consumption by 2020 [2]. In 2018, the share of renewable energy sources in final energy consumption

in the EU was 18.9%, compared to 9.6% in 2004 [3]. Although the EU as a whole is in a good position to meet its 2020 goals, some member states will have to make additional efforts to fulfil their obligations regarding the overall share of renewable energy in gross final energy consumption. There seems to be a large disproportion between renewable energy sources share in total electricity production in individual EU member states. In 2018, renewable energy reached more than half (54.6%) of the gross final energy consumption in Sweden. It was the first country among EU member states to achieve that goal, far ahead of Finland (41.2%), Latvia (40.3%), Denmark (36.1%), and Austria (33.4%). Countries with the lowest share of renewable energy were at the end of this ranking. These were the Netherlands (7.4%), Malta (8.0%), Luxembourg (9.1%), and Belgium (9.4%). The targets for these countries require an increase in the share of renewable energy in final energy consumption. In Poland it was 11.3% in 2018 in comparison to the goal of 15% by 2020—relatively far from the requirements.

An increase in the share of renewable energy sources in total electricity production requires building new renewable energy source installations based on available technologies, or improvement of the efficiency of the existing ones. One of the sources of renewable energy is biogas obtained from biogas plants. According to the latest Statistical Report 2019 on Biogas [4], gross energy consumption from biogas in Europe has increased 25 times since 1990. The steady upward trend confirms the potential and capabilities of biogas, even greater in recent years due to the development of advanced technologies and cheaper components for installations (fermentation chambers or units for the conversion of raw biogas to biomethane injected into the gas network). As much as 71% of biogas plants in Europe are fed agricultural substrates (energy crop silage, liquid manure, agricultural wastes). The demand for these types of installations is still high, particularly because the production of biogas from agro residue/agro waste along with organic recycling of digestate is an example of good practice in the area of circular economy.

In order to make better use of biogas plants, in other words, to increase biogas production, scientists around the world attempt to use various technologies [5–7]. One of them is the application of hydrodynamic disintegration (HD) of substrate directed to fermentation chambers. This method provides for lower energy consumption compared to other pre-treatment methods [8,9] and therefore offers a better chance of achieving a positive energy balance. Hydrodynamic disintegration has previously been successfully used for disintegration of sewage sludge [8,10,11]. This has led to attempts to use HD in the pre-treatment of feedstock in agricultural biogas plants, although reports regarding this are still scarce [9,12,13].

The possibility of increasing the amount of methane produced with a positive energy balance in agriculture biogas plant was demonstrated by Garuti et al. [9]. Biochemical methane potential (BMP) test results documented a 2.9%, 3.5%, and 14.0% increase in methane yield for hydrodynamic disintegration with the following energy inputs: 954 kJ/kg TS (total solids), 470 kJ/kg TS and 740 kJ/kg TS. Full-scale experiments have shown 17% lower electrical energy consumption (for 470 kJ/kg TS) due to higher biogas production. The cited authors used pig slurry and energy crops (maize silage and triticale silage) as feedstock, and agricultural by-products (beet molasses, and corn meal) as supplementary biomasses. Hydrodynamic disintegration was also used to pre-treat *Sida hermaphrodita* silage mixed with cattle manure [13]. An increase in methane production by 14.7% and 29.4% was obtained with an energy profit of 0.14 Wh/g TS and 0.17 Wh/g TS for HD conducted in 2.5 min and 5 min, respectively. The comparison of hydrodynamic and ultrasonic disintegration as pre-treatment of cattle manure mixed with wheat straw has been presented in [12]. As a result of both methods, a similar increase in biogas production rate was obtained, reaching 18.5 m³/d and 19.8 m³/d, respectively. A similar increase was also observed in cumulative biogas yield—from 369 L/kg VS (volatile solids) (without pre-treatment) to 430 L/kg VS (hydrodynamic disintegration pre-treatment) and 460 L/kg VS (ultrasonic disintegration pre-treatment). The net energy output for a system with HD (61.05 kWh/d), however, was higher than that for a system with sonification (52.15 kWh/d). Along with the application of HD to increase the efficiency of anaerobic digestion, the process is also tested for the valorisation

of lignocellulosic biomass for ethanol production [14], biodiesel production from Thumba oil [15], removal of toxic substances [13], and microalgae cells disruption [16].

This paper presents the process of adaptation of a hydrodynamic disintegration device from working with sewage sludge (HDS, hydrodynamic disintegrator for sludge), previously described in reference [17], to technology working with a broad spectrum of agricultural substrates, as well as the testing procedures. Meeting the study objective involved three stages. First, mathematical modelling was carried out to generate design guidelines. The primary elements distinguishing it from the device working with sewage sludge are additional shredding knives and ribs that help grinding/breaking up agricultural substrates. In the disintegrator, a pressure gradient is created in the rotor spaces as a result of centrifugal force. In active zones located closest to the axis of rotation, the fluid pressure drops below the evaporation pressure at a given temperature. As a result, vapour-gas bubbles are formed in the zone of the lowest pressure, and disappear in the zone of high pressure, which is called cavitation. This phenomenon causes biomass disintegration. The second stage involved production of the device (HDA). The third stage focused on conducting research and testing of the device. Maize silage (MS), a substrate commonly used in agricultural biogas plants, was chosen for the research. Disintegration of this substrate in the device dedicated to sewage sludge caused operation problems, namely clogging the rotor openings and shutting off the device. Another serious challenge of this study was the determination of the operating parameters of the device that would ensure not only an increase in methane production, but also a positive energy balance.

2. Methods

2.1. Modelling

The modelled process is turbulent flow of agricultural substrates in the disintegrator's domain in which cavitation is suspected. The modelling part covers a system of equations used for flow description, as well as the assumptions and model implementation part presenting the geometry, mesh, and solver settings.

2.1.1. Mathematical Model

Few studies have focused on mathematical modelling of hydrodynamic disintegration of agricultural substrates so far. It may have resulted from the challenges of modelling of the wide range of inhomogeneous mixtures the composition of which can vary in time.

That is why water is a commonly used medium in mathematical modelling of hydrodynamic disintegration devices [18,19] (among the others approaches presented). Water is also a frequently used medium for real device testing [20–23]. Being aware of the simplification resulting from the intake of water and taking into account numerous difficulties occurring in the modelling of agricultural waste substrate, water was also assumed as the modelled liquid in this study. Water was modelled as continuous liquid, fulfilling the mass conservation equation. Heat transfer calculations employed the total energy equation [24], including the viscous work term. The momentum conservation principle in turbulent flow involved the application of the Reynolds averaged Navier–Stokes equation (RANS). This equation requires the implementation of additional functional relationships between Reynolds stresses or effective coefficients, and averaged field parameters determined by the turbulence model.

Models most commonly used for this purpose are $k-\varepsilon$ and $k-\omega$ models (both with certain modifications) [25–27]. The majority of turbulent flow descriptions can successfully apply the standard $k-\varepsilon$ model. It is characterised by reasonable accuracy for a broad variety of flows, as well as adequate calculation time. Unfortunately, the $k-\varepsilon$ model does not deal well with flow description in non-equilibrium boundary layers [28]. In contradiction to $k-\varepsilon$, the $k-\omega$ model calculates the turbulent energy dissipation rate (ω) instead of the dissipation equation. The $k-\omega$ model is dedicated to the circulation of near-wall region flows, even with significant pressure gradients in the wall's vicinity. Drawbacks of the $k-\omega$ model include strong sensitivity to ω values in the freestream far from the

boundary layer [29]. To face this challenge, the shear stress transport (SST) version of $k-\omega$ was developed. In this case, the $k-\varepsilon$ model is used in free stream regions [30]. For flow modelling via the domain with the rotor, the $k-\varepsilon$ model is typically applied, as described in Ref. [31–33], so it was selected for the turbulence calculation in the whole fluid domain in this study.

Cavitation is suspected in the analysed flow. The stochastic model of this phenomenon in turbulent flow is presented in reference [34]. Article [35] covers the system of equations describing bubble stable cavitation in water, as well as bubble behaviour simulation. The mathematical model of cavitation, presenting the isothermal two-phase flow behaviour, is described in reference [36]. The numerical analysis of cavitation of water flow in Ansys Fluent in various domains is shown in reference [37].

Because the mathematical model of processes occurring in agricultural substrates disintegration is poorly described in the literature, an analogous example of cavitation in pumps can be mentioned [38]. The example of the computational fluid dynamics (CFD) model of processes occurring in the centrifugal pump is described in [39]. This study involving cavitation modelling implemented the Rayleigh–Plesset equation. Because cavitation modelling is a complicated and time-consuming process, it was not modelled directly in this study. The cavitation zones were determined through the identification of low pressure areas. This approach was presented, namely, in reference [24].

2.1.2. Model Implementation

The model implementation consists of three main parts: geometry designing, mesh generation, and implementation of boundary conditions and solver settings. As mentioned before, the sewage sludge disintegrator was designed in the scope of previous works, published in references [17,40]. The device was adjusted for agricultural substrates disintegration by adding shredding knives (Figure 1). Moreover, implementation of ribs was proposed to create another disintegration zone (Figure 2). The accelerated fluid at the outlet of the rotor faces the ribs, causing rapid velocity decrease contributing to the disintegration of the substrate. For the purposes of assessment of the new design, one of the objectives of this study was the comparison of the performance of two designs.

The computational grid was generated for the presented domain. For this purpose the automatic method was used. The face maximum size was set to 0.005 m. Additional face sizing (0.003 m) was applied on the rotors' surfaces, to obtain more occurrence results as the most dynamic processes are predicted there. Main mesh parameters are presented in Table 1. The applied mesh is presented in Figure 3.

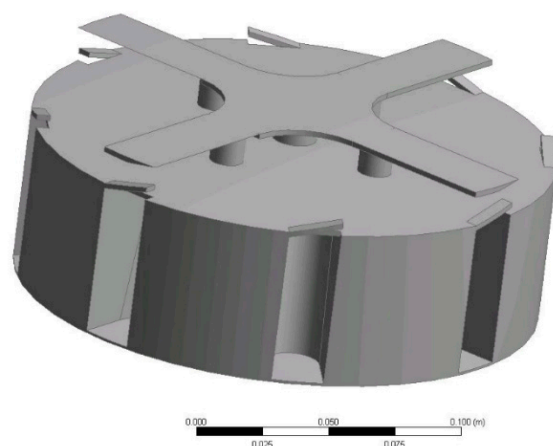


Figure 1. Adjusted rotor geometry.

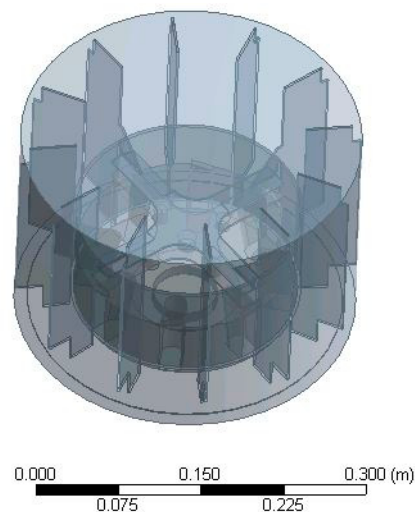


Figure 2. Fluid domain.

Table 1. Main mesh parameters.

Number of Elements	Number of Nodes	Average Quality	Average Aspect Ratio	Average Skewness
1,395,719	261,127	0.84047	1.846	0.21973

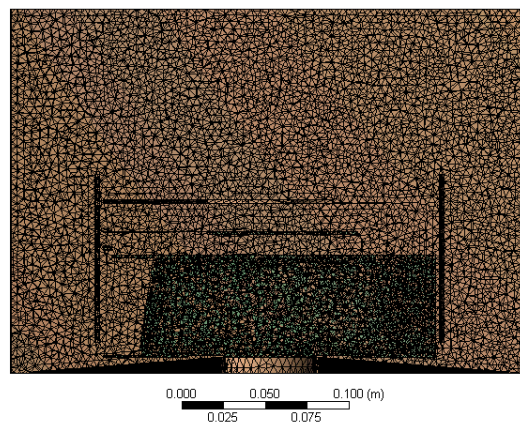


Figure 3. Mesh cross section.

The calculations were conducted with the application of available commercial software (Ansys CFX 18.2, Canonsburg, PA, USA). The rotational speed was assumed as 50 rps. As in similar cases in the literature [41], the immersed solid method was implemented. All walls were treated as adiabatic. The pulse mode of the device was considered so device filling and emptying were neglected, which is why neither inlet nor outlet were defined in the model. The transient model of the analysis was used. The total simulation time equalled 0.04 s (two full turns) with a single timestep length of 0.000111 s. Reference temperature was set to 293 K. The high resolution advection scheme option was selected. The second order backward Euler transient scheme was applied. Turbulence numerics were calculated as the first order. The root mean square (RMS) was selected for convergence criteria, and set at the level of 10^{-4} .

2.2. Appraisal of Device Operation

2.2.1. Substrate

As already mentioned in the introduction to the appraisal of the operation of the constructed device, maize silage was selected for the study as a substrate commonly applied in agricultural biogas plants. In 2019 in Poland, 420,714.003 t of MS was processed. It is the fourth most commonly applied substrate in Polish agricultural biogas plants out of 36 substrates finding application in such installations [42]. The maize silage used in the study was obtained from an agricultural biogas plant in the Lublin voivodeship (Poland). Total solids (TS) and volatile solids (VS) concentration in MS were in a range of 31.1–41.2% and 29.9–39.6%, respectively.

Before commencing the implementation of the process of hydrodynamic disintegration, the maize silage (Figure 4a, raw MS) was shredded by means of a kitchen blender with a shredding function in order to eliminate the presence of long fibres that occurred in samples collected from the prism (Figure 4b, shredded MS). Then, MS was diluted with tap water to total solids concentration at a level of approximately 5%. TS concentration in the samples used in the hydrodynamic disintegration process was 4.45–5.22% (Figure 4c, hydrated MS).



Figure 4. Maize silage: (a) Raw maize silage; (b) shredded maize silage; and (c) hydrated maize silage used in the hydrodynamic disintegration process.

2.2.2. Disintegration Batch Test

The objective of disintegration batch tests was verification whether the modified device (HDA) permits conducting disintegration of maize silage with no operation problems that occurred in the case of the device constructed for the purpose of disintegration of sewage sludge (HDS), and analysis of solubilisation of MS as a result of hydrodynamic cavitation (based on changes in the concentration of soluble chemical oxygen demand (SCOD) and volatile fatty acids (VFA)).

The disintegration batch test involved subjecting MS to the hydrodynamic disintegration process at the adopted energy density levels (E_L), in other words, a value illustrating energy use in reference to 1 L of the disintegrated medium (kJ/L), and analysis of the value of physical-chemical indicators in the samples before and after disintegration. Each test was conducted at six levels of E_L in a range of 35–210 kJ/L with a 35 kJ/L step. Conducting the process with strictly specified energy use was possible due to continuous measurement of electricity consumption coupled with the automatic system that shut off the device after the introduction of the predefined portion of energy to the disintegrated medium. Immediately after that, the temperature was measured of the disintegrated sample, and the liquid phase was separated, then subjected to the determination of the concentration of dissolved organic compounds expressed in the SCOD, as well as VFA concentration. The obtained results provided the basis for the calculation of the efficiency of organic compounds release (E_{SCOD_AW}), and the efficiency of volatile fatty acids release (E_{VFA_AW}) [43].

The study was conducted in four repetitions (R) of disintegration batch tests, each time on a different batch of maize silage. The tests were described as MS.R1, MS.R2, MS.R3, and MS.R4.

2.2.3. Biochemical Methane Potential Tests

The objective of BMP tests was the assessment of the possibility to increase the specific methane production (*SMP*) of maize silage as a result of application of the hydrodynamic disintegration process as a pre-treatment method.

BMP tests employed the Automatic Methane Potential Test System (AMPTS II). The device is composed of 15 glass bottles (test reactors), each with a total volume of 650 mL. The following was introduced to a single reactor: (i) 400 mL inoculum, namely digestate originating from the same biogas plant as the maize silage; and (ii) substrate, namely, disintegrated and non-disintegrated maize silage, in a quantity resulting in substrate load on inoculum of 5 g VS of MS per L inoculum. Tests for particular samples were performed in triplicates. Therefore, a single experiment permitted the determination of *SMP* for untreated MS, and for samples of MS disintegrated at three energy density levels (in order to determine *SMP*, observations of methane production in triplicate were also conducted for the inoculum). All test reactors were equipped with mechanical rotors operated automatically. This permitted stirring the content of the reactors for 20 s every 10 min throughout the duration of the tests. The reactors were placed in a water bath, allowing for maintaining the temperature of anaerobic digestion at a constant level. In the experiment, the value of the index was 37 °C. For the purpose of providing anaerobic conditions, the entire system was rinsed with pure nitrogen gas. Each test reactor was connected with Tygon tubing with a scrubber containing 3 M solution of sodium hydroxide with 0.4% thymolphthalein for absorbing CO₂, and then with a measurement cell measuring the volume of produced methane (it is automatically converted to standard temperature (273.15 K) and pressure (1 bar)). In the conducted experiments, the anaerobic digestion process was conducted until the daily methane production over three subsequent days was lower than one percent of total production [44]. The RIR Tukey test was used to determine the sensitivity of differences (level of sensitivity: $\alpha = 0.05$) between *SMP* determined for particular samples (STATISTICA 13.1 PL).

The scope of the study covered conducting two experiments. It was assumed that in the first experiment (described as MS-E1), maize silage would be subject to the disintegration process at energy density values of 35 kJ/L, 70 kJ/L, and 140 kJ/L, and the obtained results would provide the basis for the selection of energy density at which the disintegration process would be conducted in the subsequent experiment (MS-E2), with consideration of striving to obtain a positive energy balance.

2.2.4. Analytics

The chemical analyses (*SCOD*, *VFA*) were performed in accordance with standard analytical procedures (APHA) with the application of a spectrophotometer (DR3900, Hach Lange, CO, USA). The liquid phase of the analysed samples was obtained through 30 min rotation at 15,000 rpm (MPW Med.Instruments, MPW-352, Warsaw, Poland), and high-pressure filtration through membrane filters with a pore diameter of 0.45 µm (Merck Millipore, Burlington, MA, USA). *TS* and *VS* were determined using gravimetric methods in accordance with norms PN-EN 15934:2013-02 and PN-EN 15935:2013-02, respectively.

3. Results

3.1. Modelling

The comparative analysis covered two geometries of the device (original variant, without shredding knives; modified variant, with shredding knives) with a rotor diameter of 200 mm at nominal rotational speed of 3000 rpm. The scope of work implemented for the purposes of this article included no calculations for the HDS device, but only for the HDA. Results for the HDS device were implemented in the scope of earlier studies, and were presented in reference [40]. The presented analysis aimed at the determination of the effect of application of additional shredding elements on the distribution of pressure and speed in working spaces of the rotor. The character of flow in the zone of liquid outflow from the rotor in the vicinity of the ribs was also determined. The results are presented

in Figure 5 as pressure fields on the rotor surface, and liquid speed vectors. The presented simulation results show that in both cases a decrease in pressure below saturation pressure (1705 Pa, lower limit of the scale in the figures) was observed in the rotor area. Cavitation zones have an approximate size, the HDA to HDS low pressure zones volume ratio is equal to 84.64%; therefore, no significant negative effect of the introduction of shredding knives on the pressure distribution in working spaces of the rotor was observed. Despite the flow character change around the rotor caused by the needed modification implementation (shredding knives), it can be concluded that the rotor is still able to create a low pressure zone of satisfactory size. In the modified variant, a change in the character of flow above the rotor was also observed. An increase in pressure at the rib base, at the outlet from the rotor, suggests the existence of the impact zone, where disintegration of substrates can also occur, as presented in Figures 6 and 7. Moreover, the geometry with the existing knives and counter knives is characterised by increased pressure on the lateral wall of the rotor.

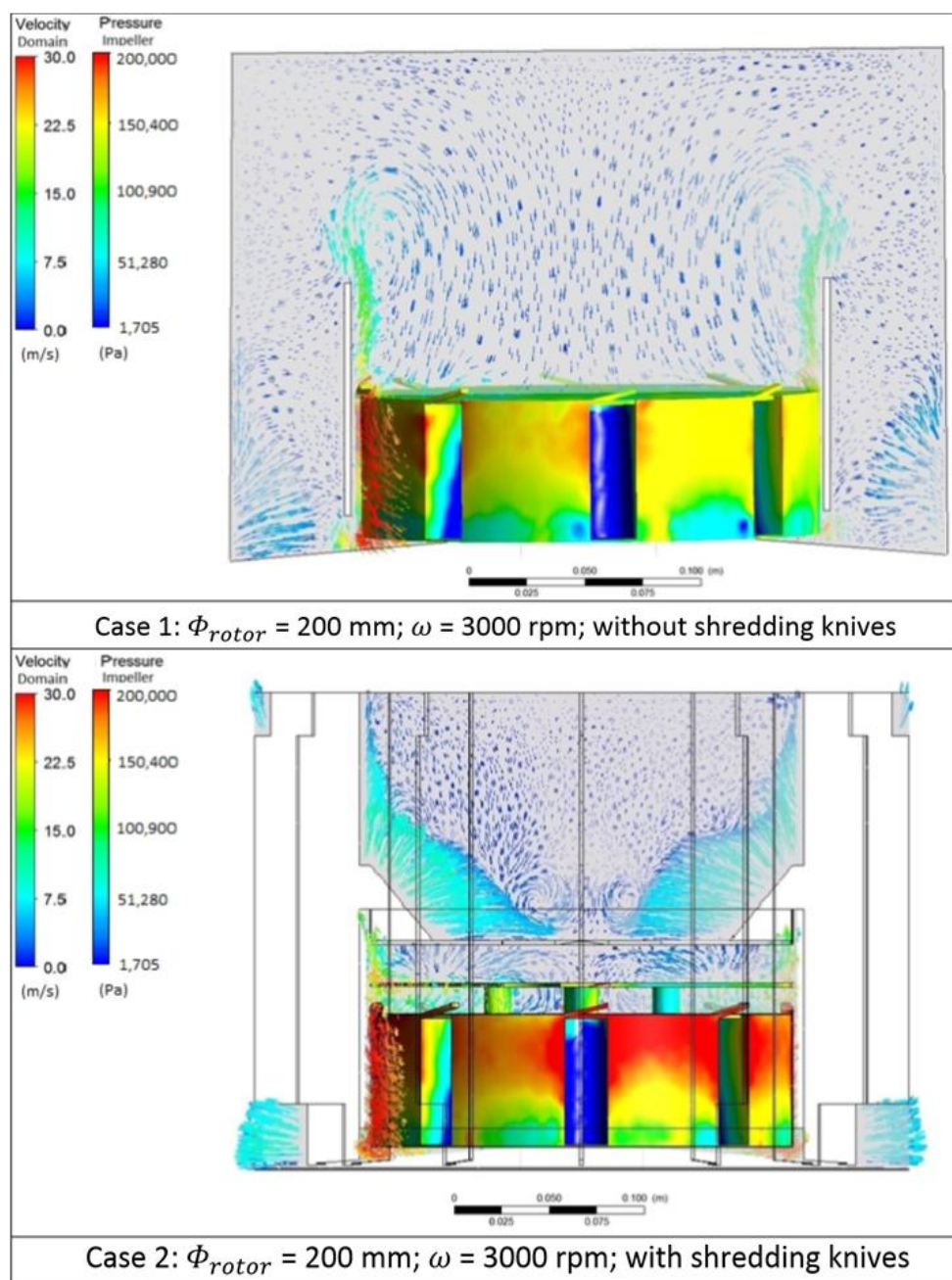


Figure 5. Comparison of pressure fields and speed fields in both variants of the device.

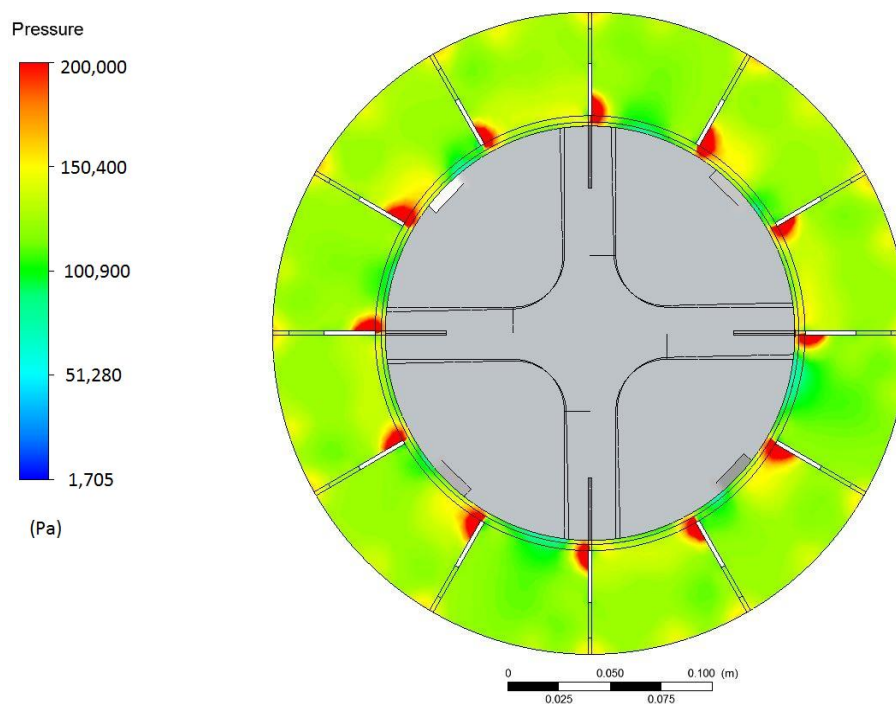


Figure 6. Pressure contour at the outlet from the rotor of the device in the modified variant.

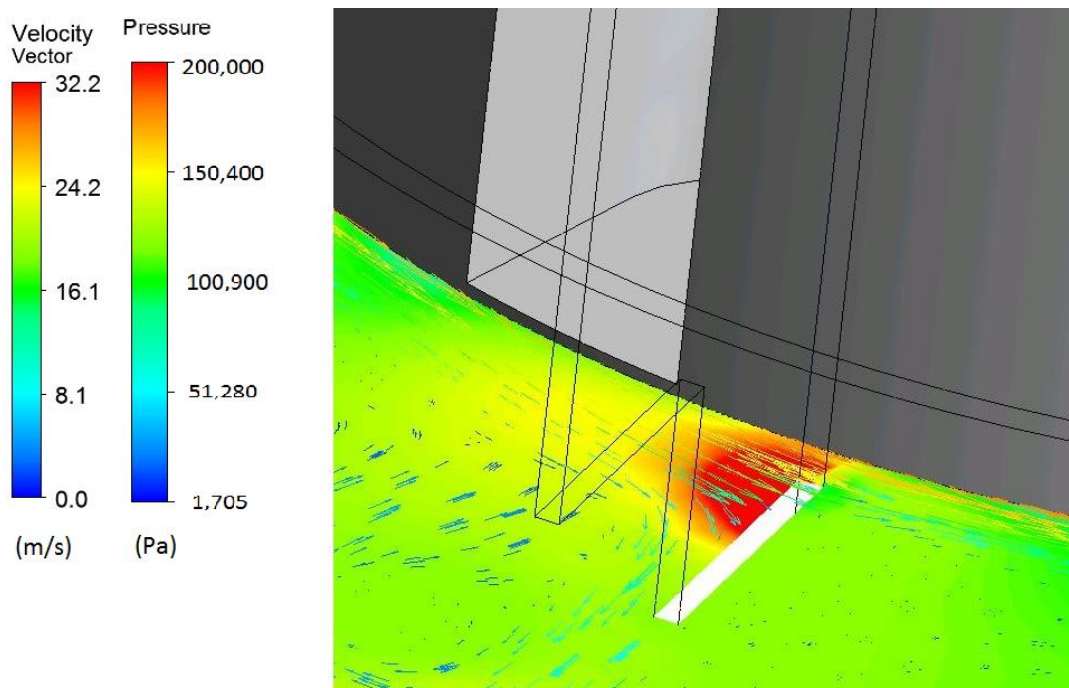


Figure 7. Pressure contour at the outlet from the rotor of the device in the modified variant, zoom-in to the outlet zone.

The obtained simulation results confirmed the lack of negative effect of the implementation of the system of shredding knives on the potential of generating cavitation in working spaces of the rotor. Due to this, and to the necessity of disintegration of agro substrate before their introduction to the rotor, introducing the solution to the modified device (HDA) is recommended.

The zones of liquid impact observed in the modelling results, manifested in a rapid pressure increase in the basal zone of the ribs, also suggest a positive effect of introducing the modification to

the disintegration of the biological structures of the substrate. The cited results provided the basis for the commencement of design of the HDA device.

The modified disintegrator (HDA) is a double cylinder circulation rotor device (Figure 8). The effect of the introduction of additional elements such as shredding knives (active, constituting an integral part of the rotor), counter knives (passive), and passive ribs is a change in the character of flow in the space above the rotor to more turbulent, and in the vicinity of the outlet of the medium from the rotor area to that generated by highest pressure difference. Therefore, two zones of disintegration exist: cavitation (rotor) and impact zone (bases of passive ribs), intensified due to the presence of circulation in the working space of the device (the medium flows through the disintegration zones several times in a cycle). Moreover, the presence of active and passive elements above the rotor disintegrates solid elements contained in the medium, allowing for the device's broader range of operation and higher tolerance to inhomogeneous mixtures.

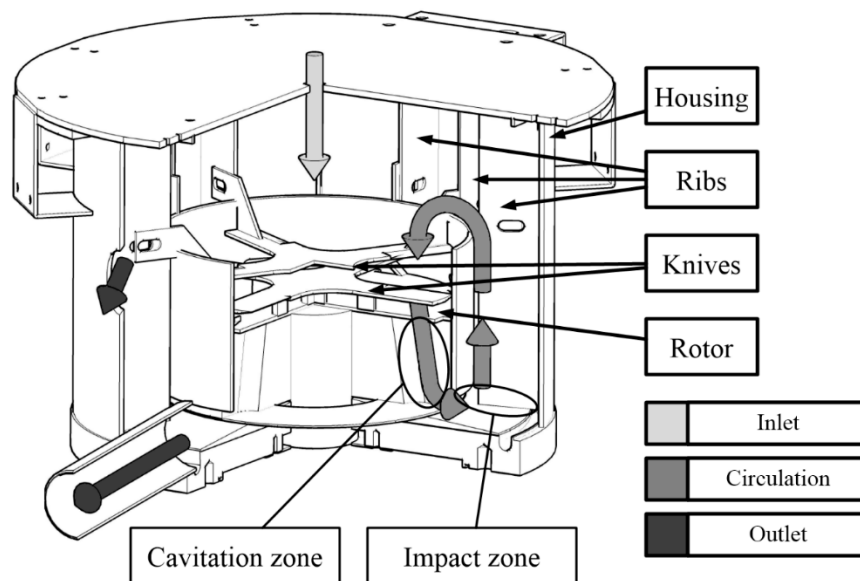


Figure 8. Diagram of the disintegrator.

3.2. Appraisal of Device Operation

No clogging of rotor openings or spontaneous shutting off of the device, in other words, problems that occurred during tests in the device constructed for disintegration of sewage sludge (HDS), were recorded in the process of hydrodynamic disintegration of maize silage in the modified device (HDA). Whereas the HDS device could be successfully used for disintegration of sewage sludge and the following substrates used in agricultural biogas plants: cow and pig slurry, remains of fruit, sugar beet pulp, and sugar beet pellets [43,45], it did not permit conducting the disintegration process of substrates such as maize silage, manure, plant waste, or straw.

The operation of the modified disintegrator was verified in the broad range of energy density of 35–210 kJ/L which in reference to TS of disintegrated maize silage corresponded to specific energy (E_S) in a range of 706–4715 kJ/ TS . For this purpose, four disintegration batch tests were conducted, involving monitoring of changes in temperature and dissolved organic compounds ($SCOD$, VFA). Lack of operation problems allowed for a transition to the next stage of the study aimed at the assessment of the possibilities to increase the methane potential of MS as a result of hydrodynamic disintegration conducted in device HDA with a positive energy balance.

3.2.1. Temperature

As suggested by data presented in Table 2 and Figure 9a, an increase in energy introduced in the process of hydrodynamic disintegration of MS was accompanied by a gradual, almost linear increase

in temperature from 21.5 ± 1.4 °C for untreated samples to 55.6 ± 0.7 °C for samples disintegrated at $E_L = 210$ kJ/L (E_S : 4233–4715 kJ/TS). An approximate increase in temperature with an increase in energy supplied to the system was observed during the disintegration of sewage sludge conducted with the application of an identical rotor, but without the modification introduced for processing of substrates used in agricultural biogas plants [17]. Further batches of MS disintegrated with differing energy densities were, however, characterised by a much lower change in temperature at each E_L than that recorded for sewage sludge (MS: standard deviation in a range from ± 0.5 to ± 1.9 °C, which constituted from ± 0.9 to $\pm 6.4\%$ of particular mean values; sewage sludge: standard deviation from ± 2.4 to ± 5.5 °C, which constituted from ± 9.5 to $\pm 27.4\%$ of particular mean values). In hydrodynamic cavitation, an increase in temperature results from generation and then implosion of microbubbles filled with vapour or gas, resulting in generation of heat [46].

Table 2. Disintegration effect with a given level of energy density for maize silage.

Energy Density (kJ/L)	Duration of Hydrodynamic Disintegration (min:sec)	Temperature (°C)	SCOD (mg/L)	VFA (mg/L)	E_{SCOD_AW} (mgSCOD/kJ)	E_{VFA_AW} (mgVFA/kJ)
0 (untreated)	-	21.5 ± 1.4	4660 ± 1957	760 ± 427	-	-
35	00:41 ± 00:04	27.0 ± 1.7	7487 ± 1650	1377 ± 841	80.8 ± 37.0	17.6 ± 2.9
70	02:03 ± 00:12	35.6 ± 1.1	7450 ± 1192	1263 ± 832	39.9 ± 22.2	7.2 ± 7.2
105	04:04 ± 00:26	42.4 ± 1.9	7700 ± 1113	1248 ± 740	28.6 ± 18.4	4.0 ± 3.7
140	06:48 ± 00:41	46.0 ± 1.5	7379 ± 1239	1059 ± 856	19.4 ± 18.4	2.1 ± 4.0
175	09:57 ± 02:02	53.5 ± 0.5	7430 ± 2157	1261 ± 1028	15.6 ± 13.5	2.5 ± 3.9
210	13:07 ± 04:05	55.6 ± 0.7	7943 ± 1220	1001 ± 577	15.5 ± 11.5	0.8 ± 0.8

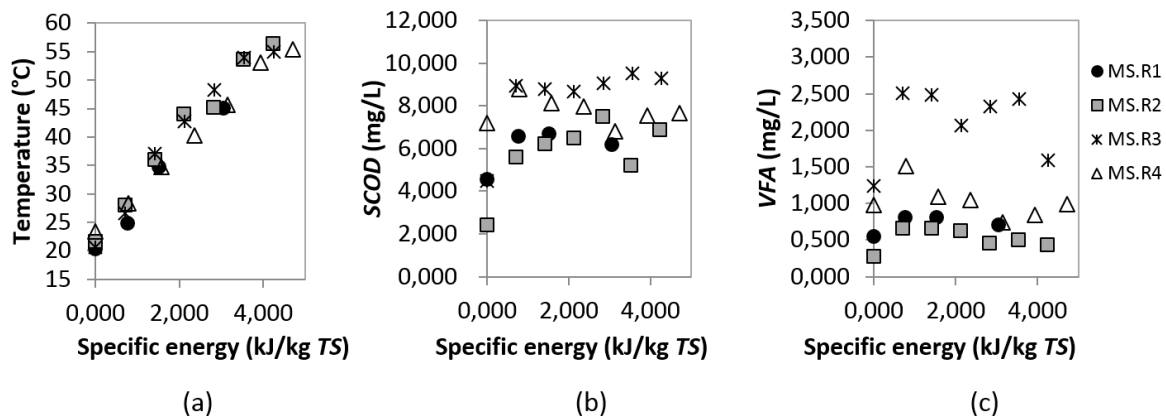


Figure 9. Effect of specific energy on: (a) Temperature of maize silage; (b) SCOD; (c) VFA release from maize silage.

3.2.2. SCOD and VFA

The comparison of values of SCOD and VFA concentrations obtained in subsequent samples disintegrated at increasing energy use shows that only after the introduction of the first portion of energy ($E_L = 35$ kJ/L), the concentration of dissolved organic compounds expressed as SCOD and VFA considerably increased (Table 2, Figure 9b,c). Values of the indicators increased by $74.8 \pm 50.2\%$ and $86.2 \pm 41.5\%$, respectively, in comparison to untreated MS, allowing for obtaining the efficiency of SCOD and VFA release in a range of 45.9–128.1 mg SCOD/kJ and 7.7–36.5 mg VFA/kJ, respectively. E_{SCOD} and E_{VFA} determined for disintegrated samples at the remaining energy density levels ($E_L \geq 70$ kJ/L) were lower by 40.8–106.2% and 50.4–111.2%, respectively. The obtained results suggest that as a result of the HD process conducted at $E_L = 35$ kJ/L, organic compounds constituting biomass building material were solubilised with simultaneous generation of easily biodegradable organic compounds. A further increase in E_L resulted in only a slight increase or decrease in the SCOD value (from 22.7 to 33.4% in

comparison to the sample disintegrated at 35 kJ/L), and a decrease in VFA concentration (from 0.2 to even 51.3% in comparison with the sample disintegrated at 35 kJ/L). The recorded decreases in SCOD and VFA values could have been related to the occurrence in the disintegrator of temperatures locally higher than boiling temperature of VFA, resulting in potential evaporation of a part of already released VFA. Loss of dissolved organic compounds could also have resulted from their oxygenation caused by free radicals $H\bullet$ and $\bullet OH$ produced in the process of hydrodynamic cavitation [47].

The course of changes in SCOD concentration in the process of hydrodynamic disintegration of MS can be compared to changes in the concentration of carbohydrates obtained as a result of hydrodynamic disintegration of *Sida hermaphrodita* silage [13]. At the beginning stage of disintegration (up to 10 min, corresponding to $E_s = 2016$ kJ/kg TS), an increase in the concentration of carbohydrates in the liquid phase was obtained, followed by the observation of no considerable increase in the concentration of the compound in the liquid.

The comparison of results of disintegration tests conducted for maize silage to results obtained for sewage sludge [17] reveals that maize silage is characterised by considerably lower susceptibility to the solubilisation process as a result of HD. In the case of sewage sludge, an increase in SCOD and VFA concentrations in disintegrated samples referred to values obtained in untreated samples varied from 110–456% at $E_L = 35$ kJ/L to 1288–3540% at $E_L = 210$ kJ/L for SCOD and from 42.5–170% at $E_L = 35$ kJ/L to 627–1084% at $E_L = 210$ kJ/L for VFA [17], whereas for maize silage it reached the following values: for SCOD 22.3–132% at $E_L = 35$ kJ/L and 6.5–185% at $E_L = 210$ kJ/L, and for VFA 49.8–137% at $E_L = 35$ kJ/L and 0.8–53.2% at $E_L = 210$ kJ/L.

3.2.3. Specific Methane Production (SMP)

In the first experiment (MS-E1), BMP tests were conducted for untreated MS and for MS subjected to the hydrodynamic disintegration process at the following energy density levels: 35 kJ/L, 70 kJ/L, and 140 kJ/L (subsequent tests were described as MS_35 kJ/L, MS_70 kJ/L, and MS_140 kJ/L), corresponding to specific energy of 797 kJ/kg TS, 1518 kJ/kg TS, and 3125 kJ/kg TS. A statistically significant increase in SMP values suggesting an increase in the susceptibility of maize silage to the anaerobic digestion process due to the applied processing method was only recorded in the case of test MS_35 kJ/L. The value of the analysed index increased by 14.6% in comparison to untreated MS (Table 3). It is worth emphasising that a similar 14.0% increase in SMP value at an approximate value of $E_s = 740$ kJ/kg TS was obtained by Garuti et al. [9] (Table 3). MS disintegration at $E_L = 70$ kJ/L caused an inconsiderable, not statistically significant increase in the methane potential of only 3.31% (Table 3). MS disintegration at $E_L = 140$ kJ/L did not contribute to an increase in SMP of the substrate. Study results of Garuti et al. [9] suggest that one of causes of a decrease in the SMP value in tests MS_70 kJ/L and MS_140 kJ/L in comparison to test MS_35 kJ/L could have been the reflocculation phenomenon involving reconnecting of disintegrated particles resulting in a decrease in the bioavailability of organic matter. The formation, as a result of the applied pre-treatment, of by-products constituting strong inhibitors of the anaerobic digestion process: (i) dissolved phenol and hemicellulose compounds (furfural, hydroxymethylfurfural); and (ii) products of the Maillard reaction such as amino acids and carbohydrates, could have been another cause of a decrease in the SMP value [9].

Table 3. Effect of hydrodynamic disintegration on specific methane production of feedstocks used in an agriculture biogas plant—literature review and results obtained in this study.

Feedstocks	Parameters of the HD Process	Working Volume of the Reactor	Temperature of Anaerobic Digestion Process (°C)	SMP (NmL/gVS)	Increase in SMP Relative to Untreated Sample (%)	References
wheat straw	untreated	500 mL	37	31.8	–	Patil et al. [48]
	(2 min, 7.5 kW, 2300 rpm)			77.9	144	
cattle manure and straw wheat	untreated	20.9 m ³	35	369 ¹	–	Zieliński et al. [12]
	4 kW, 2800 rpm			430 ¹	16.5	
<i>Sida hermaphrodita</i> silage	untreated	400 mL	37	340	–	Zieliński et al. [13]
	504 kJ/kg TS			390	14.7	
	2988 kJ/kg TS			440	30.0	
pig slurry, energy crops (maize silage and triticale silage), and agricultural by-products (beet molasses and corn meal)	untreated	1.35 L	38	139.4	–	Garuti et al. [9]
	470 kJ/kg TS			144.1	3.50	
	740 kJ/kg TS			159.1	14.0	
	954 kJ/kg TS			143.4	2.90	
maize silage (MS-E1)	untreated	400 mL	37	302	–	This study
	35 kJ/L (797 kJ/kg TS)			346	14.6	
	70 kJ/L (1518 kJ/kg TS)			312	3.31	
	140 kJ/L (3125 kJ/kg TS)			302	–	
maize silage (MS-E2)	untreated	400 mL	37	366	–	
	10 kJ/L (291 kJ/kg TS)			492	34.4	
	20 kJ/L (542 kJ/kg TS)			465	27.0	
	35 kJ/L (1009 kJ/kg TS)			445	21.6	

–, no data; ¹ value of specific biogas production (SBP) (N mL/g VS).

Considering results obtained in experiment MS-E1 and striving for net energy profit in the next experiment (MS-E2), the HD process was conducted at considerably lower E_L of 10 kJ/L, 20 kJ/L, and 35 kJ/L (MS_10 kJ/L, MS_20 kJ/L, and MS_35 kJ/L), corresponding to the following E_S levels: 291 kJ/kg TS, 542 kJ/kg TS, and 1009 kJ/kg TS. A statistically significant increase in the SMP value in comparison to untreated MS was recorded for all tests in which MS before the anaerobic digestion process was subject to hydrodynamic disintegration (Table 3). The maximum SMP value of 492 NmL/g VS occurred when MS was disintegrated at the lowest of the analysed energy densities of 10 kJ/L ($E_S = 291$ kJ/kg TS). It was a value as much as 34.4% higher than that for untreated MS. Subjecting maize silage to the HD process at E_L of 20 kJ/L and 35 kJ/L caused an increase in the SMP value of 27.0% and 21.6%, respectively (Table 3). A comparable increase in SMP of 29.0% was obtained by Habashi et al. [49], conducting anaerobic digestion of hydrodynamically disintegrated oily wastewater (the disintegration process was conducted at 25 kJ/L). Zieliński et al. [13], subjecting *Sida hermaphrodita* silage to hydrodynamic cavitation, obtained an increase in methane production varying from 14.7 to 30.0%. A 144% increase in methane production in comparison to the control sample was recorded by Patil et al. [48] in wheat straw subject to the HD process (2 min, 7.5 kW, 2300 rpm).

3.2.4. Energy Balance

In order to evaluate net energy profit for both experiments (MS-E1 and MS-E2), energy balancing was performed, where the value of possible electricity obtained from additionally produced methane

was referred to the amount of energy used in the process of HD of maize silage, and the resulting index was called relative energy profit (*REP*):

$$REP = \frac{\text{Extra electricity}}{\text{Energy applied for HD}} * 100; (\%) \quad (1)$$

where *REP* is the relative energy profit, (%); Extra electricity is the amount of electricity additionally produced from methane, (Wh); and Energy applied for HD is the amount of electricity used for hydrodynamic pre-treatment of maize silage, (Wh).

In the first experiment (MS-E1), energy input for pre-treatment (HD) for each of the analysed samples exceeds the amount of energy additionally produced from methane, as evidenced by negative net energy values (Table 4). In experiment MS-E2, net energy profits of 0.84 Wh, 0.48 Wh, and 0.05 Wh were recorded for all samples for MS disintegrated at 10 kJ/L, 20 kJ/L, and 35 kJ/L, respectively (Table 4). The values of relative energy profit were 599%, 253%, and 108%, respectively for MS 10 kJ/L, MS 20 kJ/L, and MS 35 kJ/L (Table 4). It is also worth emphasising that the produced net amount of energy in sample MS 10 kJ/L considerably exceeds the amount of energy used for the HD process. Therefore, the obtained results show that the analysed disintegration method is an attractive method of pre-treatment of a substrate directed to the digestion chamber, and the application of the modified device (HDA) in an agricultural biogas plant will most probably permit obtaining a positive energy balance. Positive effects of the introduction of hydrodynamic disintegration to the agricultural biogas plant in the form of energy profit are also documented by results obtained by Garuti et al. [9] and Zieliński et al. [13].

Table 4. Energy balance.

Parameters	Unit	MS_E1			MS_E2				
		Untreated MS	MS 35 kJ/L	MS 70 kJ/L	MS 140 kJ/L	Untreated MS	MS 10 kJ/L	MS 20 kJ/L	MS 35 kJ/L
Methane energy content ¹	(Wh)	3.13	3.46	3.12	3.02	7.32	9.84	9.30	8.90
Electricity ²	(Wh)	1.25	1.38	1.25	1.20	2.93	3.94	3.72	3.56
Extra electricity ³	(Wh)	–	0.13	0.00	0.00	–	1.01	0.79	0.63
Energy applied for HD	(Wh)	–	0.23	0.42	0.91	–	0.17	0.31	0.58
Net energy production	(Wh)	–	–0.10	–0.42	–0.91	–	0.84	0.48	0.05
Relative energy profit (<i>REP</i>)	(%)	–	–	–	–	–	599	253	108

¹ Methane energy content calculated by assuming methane calorific value equal to 36 MJ/m³; ² electricity calculated by assuming electrical efficiency of engine equal to 40%; ³ Extra electricity = electricity dez. – electricity untreated, (Wh); Electricity dez., amount of electricity produced in a disintegrated sample at a predefined energy density level (Wh); Electricity untreated, amount of electricity produced in an untreated sample (Wh).

4. Conclusions

The HDS device was developed in the scope of previous works. Although HDS works properly with the sewage sludge substrate, it cannot be successfully used for agricultural waste disintegration due to different medium characteristics causing numerous operation problems such as clogging. Adjusting HDS for this purpose involved proposing several modifications, and their verification in the scope of this study. First, a system of shredding knives was added to provide substrate pre-treatment contributing to its initial fragmentation to avoid operation problems. The presented numerical analysis was conducted to verify the effect of the module's implementation on the occurrence of cavitation zones in the vicinity of the rotor, as well as its effect on flow in the domain above the rotor. No negative impact on the cavitation zones was determined. Shredding knives can be added with no disturbance of the disintegration process. Moreover, the introduction of additional elements in the recirculation zone was proposed. The study verified the potential of the implementation of ribs contributing to the development of an additional zone of substrate structure damage. The analysis results suggest the development of high pressure zones in the vicinity of the rib bases, where the rotor high-speed outflow

reaches an obstacle and its velocity rapidly decreases. This phenomenon can contribute to substrate structure damage leading to more effective disintegration. Due to the mathematical modelling results, the proposed modifications seem to improve the sewage sludge disintegrator (HDS), and extend the range of substrates that could possibly be disintegrated by agricultural substrates. Therefore, the new device design was proposed (HDA).

Results of disintegration batch tests confirmed the possibility of conducting the process of disintegration of maize silage in HDA which could not be done in HDS. The applied pre-treatment method permitted an increase in the methane potential of maize silage by 34.4%, 27.0%, and 21.6%, respectively, for samples disintegrated at energy densities of 10 kJ/L, 20 kJ/L, and 35 kJ/L with net energy profit, offering high chances for the applicability of the analysed technology at a technical scale.

Author Contributions: Conceptualization, M.Z.-S. and P.K.; methodology, M.Z.-S. and P.K.; formal analysis M.Z.-S., A.D., A.G., P.K., M.S., and J.W.; investigation, A.D., A.G., M.S., J.W., K.U., and K.S.-S.; resources, M.Z.-S., A.D., A.G., K.U., and M.W.; writing—original draft preparation, M.Z.-S., A.D., A.G., P.K., M.S., K.U., J.W., and M.W.; writing—review and editing, M.Z.-S., A.D., P.K.; visualization, A.D., A.G., M.S., J.W.; funding acquisition, M.Z.-S. All authors have read and agreed to the published version of the manuscript

Funding: The study was implemented in the scope of a research project entitled “Development of a technology for preparation substrates used in methane co-fermentation by disintegration methods” (DEZMETAN) (No.: POIR.04.01.02-00-0022/17), financed in the scope of Measure 4.1 of the Operational Programme Smart Growth 2014-2020 co-financed from the resources of the European Regional Development Fund. The language correction of the article and article processing charge were financed by the Strategic Research Project of the Warsaw University of Technology “Circular Economy” (2019/2020).

Conflicts of Interest: The authors declare no conflict of interest.

Abbreviations

AMPTS II	Automatic Methane Potential Test System
BMP	biochemical methane potential
CFD	computational fluid dynamics
E_L	energy density
ES	specific energy
ESCOD_AW	the efficiency of organic compounds release
EVFA_AW	the efficiency of volatile fatty acids release
HD	hydrodynamic disintegration
HDA	hydrodynamic disintegrator for agriculture
HDS	hydrodynamic disintegrator for sludge
MS	maize silage
R	repetition
RANS	Reynolds averaged Navier–Stokes
REP	relative energy profit
RMS	root mean square
SCOD	soluble chemical oxygen demand
SBP	specific biogas production
SMP	specific methane production
SST	shear stress transport
TS	total solids
VFA	volatile fatty acids
VS	volatile solid

References

1. Directive (EU) 2018/2001 of the European Parliament and of the Council on the Promotion of the Use of Energy from Renewable Sources. 2018. Available online: www.eur-lex.europa.eu (accessed on 30 June 2020).
2. Schöpe, M. Renewable energy directive. *Eur. Wind Energy Conf. Exhib.* **2008**, *1*, 32–38.
3. Eurostat. Share of Energy from Renewable Sources. 2020. Available online: www.ec.europa.eu (accessed on 30 June 2020).

4. Bioenergy Europe. Statistical Report 2019 on Biogas. 2020. Available online: www.bioenergyeurope.org (accessed on 30 June 2020).
5. Fernandez, H.C.; Franco, R.T.; Bayard, R.; Buffiere, P. Mechanical Pre-treatments Evaluation of Cattle Manure Before Anaerobic Digestion. *Waste Biomass Valoriz.* **2020**, 1–10. [[CrossRef](#)]
6. Bolado-Rodríguez, S.; Toquero, C.; Martín-Juárez, J.; Travaini, R.; García, P.; Rodríguez, S.B. Effect of thermal, acid, alkaline and alkaline-peroxide pretreatments on the biochemical methane potential and kinetics of the anaerobic digestion of wheat straw and sugarcane bagasse. *Bioresour. Technol.* **2016**, *201*, 182–190. [[CrossRef](#)]
7. Li, P.; He, C.; Li, G.; Ding, P.; Lan, M.; Gao, Z.; Jiao, Y. Biological pretreatment of corn straw for enhancing degradation efficiency and biogas production. *Bioengineered* **2020**, *11*, 251–260. [[CrossRef](#)]
8. Lee, I.; Han, J.-I. The effects of waste-activated sludge pretreatment using hydrodynamic cavitation for methane production. *Ultrason. Sonochem.* **2013**, *20*, 1450–1455. [[CrossRef](#)]
9. Garuti, M.; Langone, M.; Fabbri, C.; Piccinini, S. Monitoring of full-scale hydrodynamic cavitation pretreatment in agricultural biogas plant. *Bioresour. Technol.* **2018**, *247*, 599–609. [[CrossRef](#)]
10. Żubrowska-Sudoł, M.; Podedworna, J.; Sytek-Szmeichel, K.; Bisak, A.; Krawczyk, P.; Garlicka, A. The effects of mechanical sludge disintegration to enhance full-scale anaerobic digestion of municipal sludge. *Therm. Sci. Eng. Prog.* **2018**, *5*, 289–295. [[CrossRef](#)]
11. Petkovšek, M.; Mlakar, M.; Levstek, M.; Stražar, M.; Širok, B.; Dular, M. A novel rotation generator of hydrodynamic cavitation for waste-activated sludge disintegration. *Ultrason. Sonochem.* **2015**, *26*, 408–414. [[CrossRef](#)]
12. Zieliński, M.; Dębowski, M.; Kisielewska, M.; Nowicka, A.; Rokicka, M.; Szwarc, K. Cavitation-based pretreatment strategies to enhance biogas production in a small-scale agricultural biogas plant. *Energy Sustain. Dev.* **2019**, *49*, 21–26. [[CrossRef](#)]
13. Zieliński, M.; Rusanowska, P.; Krzywik, A.; Dudek, M.; Nowicka, A.; Dębowski, M. Application of Hydrodynamic Cavitation for Improving Methane Fermentation of *Sida hermaphrodita* Silage. *Energies* **2019**, *12*, 526. [[CrossRef](#)]
14. Hilaes, R.T.; Kamoei, D.V.; Ahmed, M.A.; Da Silva, S.S.; Han, J.-I.; Santos, J.C.Z. A new approach for bioethanol production from sugarcane bagasse using hydrodynamic cavitation assisted-pretreatment and column reactors. *Ultrason. Sonochem.* **2018**, *43*, 219–226. [[CrossRef](#)]
15. Pal, A.; Verma, A.; Kachhwaha, S.; Maji, S. Biodiesel production through hydrodynamic cavitation and performance testing. *Renew. Energy* **2010**, *35*, 619–624. [[CrossRef](#)]
16. Lee, I.; Han, J.-I. Simultaneous treatment (cell disruption and lipid extraction) of wet microalgae using hydrodynamic cavitation for enhancing the lipid yield. *Bioresour. Technol.* **2015**, *186*, 246–251. [[CrossRef](#)]
17. Żubrowska-Sudoł, M.; Garlicka, A.; Walczak, J.; Sytek-Szmeichel, K.; Mikołajczak, A.; Stępień, M.; Krawczyk, P.; Umiejewska, K.; Wołowicz, M. Operational characteristics of an innovative device dedicated for the hydrodynamic disintegration of sewage sludge. *E3S Web Conf.* **2019**, *116*, 00105. [[CrossRef](#)]
18. Hilaes, R.T.; Dionízio, R.M.; Muñoz, S.S.; Prado, C.A.; Júnior, R.D.S.; Da Silva, S.S.; Santos, J.C.Z.; Sanchez, S. Hydrodynamic cavitation-assisted continuous pre-treatment of sugarcane bagasse for ethanol production: Effects of geometric parameters of the cavitation device. *Ultrason. Sonochem.* **2020**, *63*, 104931. [[CrossRef](#)]
19. Mancuso, G. Experimental and numerical investigation on performance of a swirling jet reactor. *Ultrason. Sonochem.* **2018**, *49*, 241–248. [[CrossRef](#)]
20. Šarc, A.; Perdih, T.S.; Petkovšek, M.; Dular, M. The issue of cavitation number value in studies of water treatment by hydrodynamic cavitation. *Ultrason. Sonochem.* **2017**, *34*, 51–59. [[CrossRef](#)]
21. Chanda, S.K. Disintegration of Sludge Using Ozone-Hydrodynamic Cavitation. Master's Thesis, The University of British Columbia, Vancouver, BC, Canada, 2012.
22. Kim, H.; Koo, B.; Lee, S.; Yoon, J.Y. Experimental study of cavitation intensity using a novel hydrodynamic cavitation reactor. *J. Mech. Sci. Technol.* **2019**, *33*, 4303–4310. [[CrossRef](#)]
23. Tao, Y.; Cai, J.; Huai, X.; Liu, B.; Guo, Z. Application of Hydrodynamic Cavitation to Wastewater Treatment. *Chem. Eng. Technol.* **2016**, *39*, 1363–1376. [[CrossRef](#)]
24. Aman, A.; Sileshi, K.; Dribssa, E. Flow simulation and performance prediction of centrifugal pumps using CFD-tool. *J. EEA* **2011**, *28*, 59–65.
25. Bulat, M.P.; Bulat, P.V. Comparison of Turbulence Models in the Calculation of Supersonic Separated Flows. *World Appl. Sci. J.* **2013**, *27*, 1263–1266.

26. Bartosiewicz, Y.; Aidoun, Z.; Desevaux, P.; Mercadier, Y. Numerical and experimental investigations on supersonic ejectors. *Int. J. Heat Fluid Flow* **2005**, *26*, 56–70. [CrossRef]
27. Dzido, A.; Krawczyk, P.; Kurkus-Gruszecka, M. Numerical Analysis of Dry Ice Blasting Convergent-Divergent Supersonic Nozzle. *Energies* **2019**, *12*, 4787. [CrossRef]
28. ANSYS Inc. *Innovative Turbulence Modeling: SST Model in ANSYS CFX*®; ANSYS Inc.: Canonsburg, PA, USA, 2004.
29. Menter, F.R.; Kuntz, M.; Langtry, R. Ten years of industrial experience with the SST turbulence model. *Heat Mass Transf.* **2003**, *4*, 625–632.
30. Bartosiewicz, Y.; Aidoun, Z. CFD-Experiments Integration in the Evaluation of Six Turbulence Models for Supersonic Ejectors Modeling. In Proceedings of the Integrating CFD and Experiments Conference, Glasgow, UK, 8–9 September 2003.
31. Barrio, R.; Parrondo, J.; Blanco, E. Numerical analysis of the unsteady flow in the near-tongue region in a volute-type centrifugal pump for different operating points. *Comput. Fluids* **2010**, *39*, 859–870. [CrossRef]
32. Yang, S.-S.; Derakhshan, S.; Kong, F.-Y. Theoretical, numerical and experimental prediction of pump as turbine performance. *Renew. Energy* **2012**, *48*, 507–513. [CrossRef]
33. Medvitz, R.B.; Kunz, R.F.; Boger, D.A.; Lindau, J.W.; Yocum, A.M.; Pauley, L.L. Performance Analysis of Cavitating Flow in Centrifugal Pumps Using Multiphase CFD. *J. Fluids Eng.* **2002**, *124*, 377–383. [CrossRef]
34. Wilczyński, L. Stochastic modeling of cavitation phenomena in turbulent flow. *Adv. Fluid Mech.* **2000**, *29*, 503–512.
35. Man, V.H.; Li, M.S.; Derreumaux, P.; Nguyen, P.H. Rayleigh-Plesset equation of the bubble stable cavitation in water: A nonequilibrium all-atom molecular dynamics simulation study. *J. Chem. Phys.* **2018**, *148*, 094505. [CrossRef]
36. Gawin, D.; Sanavia, L.; Schrefler, B.A. Cavitation modelling in saturated geomaterials with application to dynamic strain localization. *Int. J. Numer. Methods Fluids* **1998**, *27*, 109–125. [CrossRef]
37. Linek, T.; Tański, T.; Borek, W. Numerical analysis of the cavitation effect occurring on the surface of steel constructional elements. *Arch. Mater. Sci. Eng.* **2017**, *85*, 24–34. [CrossRef]
38. Shah, S.; Jain, S.V.; Patel, R.N.; Lakhera, V.J. CFD for Centrifugal Pumps: A Review of the State-of-the-Art. *Procedia Eng.* **2013**, *51*, 715–720. [CrossRef]
39. Moloshnyi, O.; Sotnyk, M. Cavitation in centrifugal pump with rotating walls of axial inlet device. *IOP Conf. Ser. Mater. Sci. Eng.* **2017**, *233*, 012007. [CrossRef]
40. Stępień, M.; Krawczyk, P.; Mikołajczak, A.; Wołowicz, M.; Zubrowska-Sudol, M. Analiza pracy cyrkulacyjnego wirnikowego urządzenia do dezintegracji substratów biologicznych przed procesem fermentacji metanowej z zastosowaniem technik CFD. *Przemysł Chem.* **2019**, *1*, 100–102. [CrossRef]
41. Krawczyk, P.; Kurkus-Gruszecka, M.; Mikołajczak, A.; Łapka, P.; Badyda, K. Computational fluid dynamic analysis and validation of the single stage low pressure rotary lobe compressed air expander. *Therm. Sci.* **2019**, *23*, 1–10.
42. BIP KORW. Available online: <http://bip.kowr.gov.pl/informacje-publiczne/odnawialne-zrodla-energii/biogaz-rolniczy/dane-dotyczace-dzialalnosci-wytworcow-biogazu-rolniczego-w-latach-2011-2019> (accessed on 7 June 2020).
43. Zubrowska-Sudol, M.; Walczak, J.; Garlicka, A.; Sytek-Szmeichel, K.; Umiejewska, K. How to assess the efficiency of the agro waste disintegration process. *Environ. Technol.* **2020**, *12*, 1–11. [CrossRef]
44. Holliger, C.; Alves, M.M.; Andrade, D.; Angelidaki, I.; Astals, S.; Baier, U.; Bougrier, C.; Buffière, P.; Carballa, M.; De Wilde, V.; et al. Towards a standardization of biomethane potential tests. *Water Sci. Technol.* **2016**, *74*, 2515–2522. [CrossRef]
45. Zubrowska-Sudol, M.; Krawczyk, P.; Garlicka, A.; Sytek-Szmeichel, K.; Walczak, J. Implementation Report of Stage 1: Development of a Technology for Preparation Substrates Used in Methane Co-Fermentation by Disintegration Methods, (DEZMETAN) No.: POIR.04.01.02-00-0022/17. 2020. Available online: <https://biopolinex.pl/en/dezmetan-en> (accessed on 30 June 2020).
46. Zupanc, M.; Kosjek, T.; Petkovšek, M.; Dular, M.; Kompare, B.; Širok, B.; Stražar, M.; Heath, E. Shear-induced hydrodynamic cavitation as a tool for pharmaceutical micropollutants removal from urban wastewater. *Ultrason. Sonochem.* **2014**, *21*, 1213–1221. [CrossRef] [PubMed]

47. Dular, M.; Griessler-Bulc, T.; Gutierrez-Aguirre, I.; Heath, E.; Kosjek, T.; Klemenčič, A.K.; Oder, M.; Petkovšek, M.; Rački, N.; Ravnikar, M.; et al. Use of hydrodynamic cavitation in (waste)water treatment. *Ultrason. Sonochem.* **2016**, *29*, 577–588. [[CrossRef](#)]
48. Patil, P.N.; Gogate, P.R.; Csoka, L.; Dregelyi-Kiss, Á.; Horvath, M. Intensification of biogas production using pretreatment based on hydrodynamic cavitation. *Ultrason. Sonochem.* **2016**, *30*, 79–86. [[CrossRef](#)]
49. Habashi, N.; Mehrdadi, N.; Mennerich, A.; Alighardashi, A.; Torabian, A. Hydrodynamic cavitation as a novel approach for pretreatment of oily wastewater for anaerobic co-digestion with waste activated sludge. *Ultrason. Sonochem.* **2016**, *31*, 362–370. [[CrossRef](#)] [[PubMed](#)]



© 2020 by the authors. Licensee MDPI, Basel, Switzerland. This article is an open access article distributed under the terms and conditions of the Creative Commons Attribution (CC BY) license (<http://creativecommons.org/licenses/by/4.0/>).